Isotope ratio mass spectrometry and spectroscopic techniques for microplastics characterization

Quinn T. Birch[a], **Phillip M. Potter**[b], **Patricio X. Pinto**[c], **Dionysios D. Dionysiou**[a], **Souhail R. Al-Abed**[d,*]

[a]Department of Chemical and Environmental Engineering, University of Cincinnati, Cincinnati, OH, 45221, USA

[b]ORISE, USEPA, Cincinnati, OH, 45220, USA

[c]Pegasus Technical Services, Inc., Cincinnati, OH, 45219, USA

[d]Center for Environmental Solutions and Emergency Response, U.S. Environmental Protection Agency (USEPA), Cincinnati, OH, 45220, USA

Abstract

Micro- and nano-scale plastic particles in the environment result from their direct release and degradation of larger plastic debris. Relative to macro-sized plastics, these small particles are of special concern due to their potential impact on marine, freshwater, and terrestrial systems. While microplastic (MP) pollution has been widely studied in geographic regions globally, many questions remain about its origins. It is assumed that urban environments are the main contributors but systematic studies are lacking. The absence of standard methods to characterize and quantify MPs and smaller particles in environmental and biological matrices has hindered progress in understanding their geographic origins and sources, distribution, and impact. Hence, the development and standardization of methods is needed to establish the potential environmental and human health risks. In this study, we investigated stable carbon isotope ratio mass spectrometry (IRMS), attenuated total reflectance - Fourier transform infrared (ATR-FTIR) spectroscopy, and micro-Raman spectroscopy (μ-Raman) as complementary techniques for characterization of common plastics. Plastic items selected for comparative analysis included food packaging, containers, straws, and polymer pellets. The ability of IRMS to distinguish weathered samples was also investigated using the simulated weathering conditions of ultraviolet (UV) light and heat. Our IRMS results show a difference between the $\delta^{13}C$ values for plant-derived and petroleum-based polymers. We also found differences between plastic items composed of the same polymer but

from different countries, and between some recycled and nonrecycled plastics. Furthermore, increasing $\delta^{13}C$ values were observed after exposure to UV light. The results of the three techniques, and their advantages and limitations, are discussed.

Keywords

Macroplastics; Microplastic fate; Plastic waste; Polymer degradation

---

1. Introduction

The environmental occurrence and impact of nano- and microplastics (N&MPs) has attracted increasing scientific, public, and regulatory interest over the past decade. Increasing production of a myriad of plastic products is having a cumulative effect on pollution, including a diverse set of small plastic contaminants [1]. Left unchecked, environmental burdens are expected to rise sharply due to the persistence of plastics and growing environmental reservoirs. Consensus on classification of the many types and forms (macro to nano) of plastic debris is lacking. In the case of N&MPs, a definition proposed in 2008 has been used most often, which defined MPs as plastic particles <5 mm in diameter [2]. However, different upper and lower size limits for MPs have been used, with proposed lower limits at the micrometer or sub-μm range, typically >1000 nm or >100 nm. Particles with their largest dimension   these limits are considered nanoplastics. Size classifications for plastic debris have been summarized elsewhere (e.g., Ref. [2,3].

Numerous studies of N&MPs have found concerning results including N&MPs in sludge and discharge by WWTPs [4–8], contamination of freshwater and terrestrial systems [9–13], potential adverse effects on aquatic organisms [14,15], bioaccumulation and amplification in the food chain [16], sorption of toxins [17–19], ingestion and translocation [16,20,21], and the presence of MPs in human stool samples [22]. Though the pervasiveness of plastic pollution has clearly been demonstrated, major research gaps must be addressed to better understand their potential environmental and human health risks. Systematic studies of relevant environmental compartments are needed to determine the geographic origins and source, types, abundances, dispersion, and environmental transformations of N&MPs, especially of freshwater and terrestrial systems. Currently, the presence of N&MPs in the environment may be underestimated as most of the prior aquatic quantification surveys (80% in a review of 50 studies) accounted only for MPs   300 μm [23]. Hence, the advance and standardization of sizing, sampling, separation, identification and quantification methods would be highly beneficial to further the understanding of N&MPs.

Spectroscopic methods are increasingly being applied to MP analysis, the complexity of which depends on the particle size and sample matrix. Attenuated total reflectance Fourier transform infrared (ATR-FTIR) spectroscopy [24–27] has been used to identify manually sorted MPs but relatively large (>500 μm) particles are required [27]. In addition, pyrolysis gas chromatography with mass spectrometry (pyr-GC-MS) has been applied to manually sorted particles. Unsorted samples also have been analyzed by thermal-GC-MS methods

[28,29] which provide MP mass but not size or number. An overview of thermal analysis techniques was recently reported [30].

Optical microscopy coupled with spectroscopic techniques have been the most commonly applied methods for MP characterization. Techniques based on FTIR analysis have been used most often, including micro FTIR (μ-FTIR) spectroscopy [8,31–34], μ-ATR-FTIR [35–37] and μ-FTIR imaging based on FPA (focal plane array) detection [38,39]. Both μ-FTIR and ATR-FTIR can identify MPs, but the latter reportedly produced better spectra than reflectance μ-FTIR for polyethylene (PE) particles of irregular shape due to the susceptibility of the former to refractive error. Also, ATR-FTIR enabled detection of absorbance bands not observed by reflectance μ-FTIR [40]. Micro-Raman (μ-Raman) spectroscopy is another popular technique for MP identification. Microspectroscopic techniques such as μ-FTIR (transmission, reflectance modes) and μ-Raman have relatively low size limits of 20 μm and in the sub-μm range, respectively, while μ-ATR-FTIR can measure particles in the 1 mm to 70 μm range.

Combination techniques such as atomic force microscopy (AFM) coupled with FTIR and Raman spectroscopy can provide detailed information on particle morphology, in addition to particle identification, including nanoplastics [41]. Other combination techniques such as scanning electron microscopy with energy dispersive spectroscopy (SEM-EDS) also have been applied [42], and other methods continue to be developed [43]. Hyperspectral nano-IR imaging by Photo-induced Force Microscopy (PiFM), a combination of atomic force microscopy (AFM) and IR spectroscopy (with laser excitation) provides both sample topography and chemical signatures at high spatial resolution (e.g., 10–30 nm) [44]. Analytical techniques for N&MPs are discussed further in Section 3.

Although spectroscopic techniques such as FTIR and Raman are useful in classifying the types of MP pollution, they cannot necessarily identify their geographic origins or distinguish materials composed of the same polymer. Stable carbon isotope ratio mass spectrometry (IRMS) is a specialized technique that can provide information on the chemical, biological, and regional origins of materials [45]. This relatively simple technique has become routinely available and has been applied to trace the geographic origins of organic matter in the environment [45,46]. It reportedly showed promise for tracking plastic debris and changes in polymer structure due to aging and weathering processes [47,48]. The technique distinguished plant- and petroleum-derived plastics [48,49]. Because isotopic abundances in petroleum can vary with the extraction source (e.g., ^{12}C is enriched [over ^{13}C] for marine relative to terrestrial sources [50]), and results for commercial plastics can be affected by additives (e.g., stabilizers) and possibly the manufacturing process, it also may be possible to distinguish some petroleum-derived plastics. In a preliminary study, results for petroleum-derived plastics varied over a range [48]. The means for most items were similar, but several plastics could be distinguished (e.g., Teflon, acrylonitrile butadiene styrene [ABS], neoprene). High and low density polyethylene bags also differed.

Tracing the geographic origins of organic substances relies on their relative isotopic abundances. Namely, the isotope amount ratios of lighter elements common to organic substances (typically $^{13}C/^{12}C$, $^{18}O/^{16}O$, $D/^1H$, $^{15}N/^{14}N$, and $^{34}S/^{32}S$). Because isotope

amount ratios depend on local kinetic and thermodynamic factors that affect isotope enrichment or depletion, isotope signatures can be used to distinguish materials by geographic origin that otherwise have the same composition [45]. The ability to distinguish substances by geographic origin depends on retention of their isotopic composition during environmental transport, which may not always be the case. However, this information may be difficult or impossible to obtain by other methods. Because many research fields require accurate, precise measurement of the isotopic ratios of light elements, and technological advances made this type of analysis more routine, IRMS has been reliably applied to diverse fields including archaeology, biology, medicine, food authenticity, and forensics [45,46,51].

In this study, stable carbon IRMS was investigated as a complementary tool for monitoring environmental plastic debris. Isotopic signatures ($^{13}C/^{12}C$) for a variety of common plastic pollutants were determined and expressed as $\delta^{13}C$ values. In addition, ATR-FTIR and μ-Raman spectroscopies were used as complementary techniques for polymer characterization. Plastic items selected for comparative analysis included food packaging, containers, straws, and polymer pellets. Results for the three methods and their advantages and limitations are discussed. We aimed at investigating ATR-FTIR and Raman spectroscopies as tools for identifying polymers in pristine samples from different geographic origins, and complementing these analyses with IRMS $\delta^{13}C$ measurements to determine whether this technique could be useful in differentiating polymers based on feedstock (petroleum, plant-based, recycled), manufacturing site/region, and effects due to aging. This information may be useful in tracking the geographic origins and sources of plastic in the environment and aid in identifying which products and industries contribute most to plastic pollution.

2. Materials and methods

2.1. Polymer samples

The analyzed polymers were selected based on their environmental and commercial prevalence, and included pure standards, commercial pellets, and commercial products (grocery bags and food containers), some of which were recycled plastics (Table S-3). The chosen polymers were polyethylene terephthalate (PETE or PET), high- and low-density polyethylene (HDPE and LDPE), polypropylene (PP), polystyrene (PS), polyvinyl chloride (PVC), polylactic acid (PLA), acrylonitrile butadiene styrene (ABS), and polyester (PES). Samples were stored in the dark at room temperature.

2.2. Analytical techniques

We used an NC 2500 Elemental Analyzer (EA) (Carlo Erba) with a Thermo Conflo III coupled to a DeltaPlus (Thermo Finnigan) stable isotope mass spectrometer (EA-IRMS) to obtain $\delta^{13}C$ values of the studied polymers [52]. The samples were dropped by an autosampler carousel into an oxidizing furnace (chromium cobaltous oxides) at 1020 °C, where they were flash-combusted under a stream of oxygen, generating CO_2, NO_x (oxides of nitrogen), H_2O, and SO_2 if sulfur was present (further details of the instrument components are shown in Figures S-1 and S-2). We used 100–250 μg of the samples and standards (acetanilide and sulfanilamide), but it is possible to analyze smaller amounts (e.g., 20 μg) [48]. Small pieces (<4 mm largest dimension) were cut from the plastic packaging

and pellet samples and weighed in tared tin capsules. The capsules were gently crimped closed and placed in the autosampler.

The stable isotope-number ratio, R, for a substance is the ratio of the number of atoms of a heavier stable isotope to the number of atoms of a lighter one of the same chemical element in the same system [53]. In the case of carbon, R is given by the following relation:

$$R\left(^{13}C/^{12}C\right)_S = n(^{13}C)_S/n(^{12}C)_S \tag{1}$$

where n is the number of atoms of a given isotope in substance S. By convention, stable carbon isotope amount ratios $[n(^{13}C)_S/n(^{12}C)_S]$ are expressed relative to the ratio for an international standard (Pee Dee Belemnite [PDB] or Vienna PDB [VPDB]). Results are reported as $\delta^{13}C$ values, in parts per thousand (‰) (per mil), calculated as follows:

$$\delta^{13}C = \left(\frac{(R_S - R_{VPDB})}{R_{VPDB}} - 1\right) \times 1000 = \left(\frac{\left(\frac{^{13}C}{^{12}C}\right)_S}{\left(\frac{^{13}C}{^{12}C}\right)_{VPDB}} - 1\right) \times 1000 \tag{2}$$

Higher $\delta^{13}C$ values indicate enrichment of the sample in the rarer, heavier isotope, ^{13}C. The raw values for the standards and samples are blank corrected, if necessary. Also, if the standard deviation (n 3) for the standards is 0.6 ‰, no drift correction is applied. The raw (or blank-corrected) values for the standards (dependent variable) are plotted against their expected values (known). A typical r^2 for the regression curve ranges from 0.95 to 0.99 (corrective action is taken if r^2 is <0.95). A precise fit indicates complete combustion of the sample and proper operation of the EA unit. The linear regression curve is then applied to generate $\delta^{13}C$ results for the samples [52].

We used a benchtop FTIR spectrometer (Bruker Vertex-80) for polymer identification. The system (Figure S-3) was equipped with an attenuated total reflectance (ATR) accessory. A spectral library search (SEARCH package in Bruker OPUS® software) was used for polymer identification. A Renishaw inVia™ Raman microscope (Figure S-4) equipped with a Leica DM2500 microscope (x5,×50 and ×100 objectives), 633 nm laser, and Renishaw software version WiRe 3.4 was used as a complementary technique. A spectral library search was performed in KnowItAll® software (BioRad). Additional details are provided in the Supplemental Information.

2.3. Polymer aging

A short-term study of polymer degradation by heat and ultraviolet (UV) light was conducted. The following items were examined: PP and PS food packaging, white PS foam, and a PETE water bottle. Items were exposed for a one-week period under the following conditions: UV light, UV light plus water (stirred at room temperature), water only (30 °C), and heat only (40 °C). A low-pressure mercury-vapor arc lamp (5 × 5 inch grid, BHK Inc., Ontario, California, USA) was used as a source of short wavelength (254 nm and 185 nm) UV light. A paired-samples t-test was conducted to compare IRMS means ($n = 3$) for unexposed and exposed samples.

3. Results and discussion

3.1. Polymer identification by ATR-FTIR and μ-Raman

With an objective to evaluate complementary techniques for characterizing MPs and other plastic pollution, we successfully characterized all the collected samples. The constituent polymers were identified by comparison of the ATR-FTIR and μ-Raman spectra for the samples with their corresponding spectral libraries (Figures S-6 – S-20). This approach met the requirements for our study, but a custom library may be required for successful identification of plastic debris in field studies (e. g., Ref. [54,55].

The ATR-FTIR results (Fig. 1a) demonstrate accurate identification of the base polymer even in black plastics. A black food package was compared to a clear yogurt container and the lid of a black yogurt container, all of which were presumably (based on resin identification code) made of PP. Based on signature peaks, the polymer matrix was correctly identified in all three samples, in spite of the large peaks (<1050 cm^{-1}) in the ATR-FTIR spectrum of the black PP packaging material and the peak at 700 cm^{-1} in the spectrum for the black lid both not matching peaks from the chemical structure of PP. In contrast to the dark plastics, the ATR-FTIR spectrum of the clear PP container had no potentially confounding peaks. Similarly, the Raman spectrum for the clear container was as expected, but spectra for the dark items were altered. Specifically, the black lid had additional peaks (centered near 500 cm^{-1}), while the black packaging had a high background (Fig. 1b).

Although polymer additives caused additional peaks in the FTIR spectra, and additional peaks/high background in the Raman spectra, all spectral matches agreed with the polymer resin codes, confirming sample identities as necessary for the IRMS evaluation. In addition to the collected consumer goods packaging, the purchased materials (pellets) and standards also were correctly identified, including a mislabeled PE material sold as PP (Figure S-5). Thus, spectroscopic analyses were important, not only to better understand their potential limitations, but also to confirm polymer identity and provide information on the presence of additives.

3.2. Isotopic signatures by IRMS

A focus of this study was the potential utility of IRMS as a complementary tool for studies of environmental plastic debris (e.g., tracking/weathering studies). As an initial step, we needed to investigate the uniqueness of the $\delta^{13}C$ values for each polymer. To accomplish this objective, we analyzed polymer standards, commercial materials (of known polymers), and plastic items marked with a resin identification code by IRMS.

As mentioned earlier, higher (less negative) $\delta^{13}C$ values indicate a higher abundance of ^{13}C, while lower (more negative) values indicate lower amounts. Higher values are expected for plant-derived materials (e.g., bioplastics), while lower values are expected for petroleum-based plastics. Local variations in isotope amount ratios occur due to selective enrichment/ depletion of the heavier isotopes [45]. For example, plants use atmospheric or dissolved CO_2 as a carbon source, and different factors affect their ability to enrich or deplete ^{13}C from these sources, by a process called 'fractionation.' Both genetic and environmental factors (e.g., temperature, rainfall, sunlight) influence fractionation as these factors impact the

kinetics of processes such as CO_2 diffusion into the stomata of leaves [45]. The C4 plants (monocotyledons such as sugar cane, millet, corn, tropical grasses) use the Hatch–Slack photosynthetic cycle, and typically have $\delta^{13}C$ values from − 8 to − 20 ‰. In contrast, most C3 plants (dicotyledons such as wheat, rice, rye and cotton) employ the Calvin–Benson cycle and have $\delta^{13}C$ values ranging from − 22 to − 35 ‰. Crassulacean acid metabolism (CAM) plants (e.g., pineapple, cactus, orchids) can use either metabolic pathway (C3 or C4) and have $\delta^{13}C$ values between − 10 and − 34 ‰ [45]. Duarte et al. [46] applied multi-element IRMS to monitor primary producers, trace geographic origins and cycling of organic matter, and characterize the physiological status of photosynthetic organisms in the Red Sea. They reported data on carbon (and nitrogen, where possible) isotope amount ratios of phytoplankton, macroalgae, seagrasses, mangroves, and salt-marsh plants. The isotopic signatures differed among plant types across a north-south gradient. In continental plants, carbon isotope composition depended mainly on enzymatic paths of primary production (e.g., C3, C4, or CAM) and WUE (Water Use Efficiency) [46].

Suzuki et al. [49] demonstrated that stable carbon isotopic composition can be applied to discriminate plastics derived from C4 plants from those derived from petroleum. Berto et al. [48] extended this work assessing the suitability of the technique (stable carbon IRMS) to discriminate a range of plastics and natural materials, considering their use in plastic packaging items (e.g., shopping bags, water bottles). They further investigated degradation of different types of MPs in marine environments. Specifically, they examined the variation in the $\delta^{13}C$ values of plastics subjected to physical or biological processes that occur in the marine environment. Based on a preliminary field survey, they found evidence of biotic and abiotic degradation of food packaging [48].

As seen in Fig. 2, our results confirmed that PLA had a higher (less negative) $\delta^{13}C$ result than petroleum based-products. The $\delta^{13}C$ value (− 8.93 ‰) for PLA is consistent with a C4 plant origin ($\delta^{13}C$ range of − 8 to − 20 ‰), being derived mainly from corn starch (C4) in the US (or tapioca root, a cassava species with C3–C4 character, in Asia; and sugarcane [C4] elsewhere). We compared our results (means, $n = 3$ or 4 for each item analyzed) for three sample sets analyzed over several months with those reported by Berto et al. [48] (Fig. 2). The second set was analyzed about two weeks (16 days) after the first, after a system shut down for maintenance, while the third was analyzed about five months later. Overall, our results show reasonable agreement with Berto et al. [48]; except for ABS and PLA, which were lower (more negative) than our results. In one case, for a PVC powder, our result was lower than that reported by Berto et al. [48]. Our result for PVC was for triplicate analysis of a powder, while Berto et al. [48] analyzed six samples that may have been from different suppliers. Similarly, our results (means, $n = 3$) for ABS, PLA, and PC (all in pellet form) represented a single material, which also may explain the larger discrepancies for ABS and PLA. In the case of PLA, differences also may relate to different plant feedstocks. In this study, the number of items and total analyses (n) representing the mean (blue bars, Fig. 5) for a given polymer were as follows: PVC: 1 powder ($n = 3$), PE: 17 items ($n = 54$), ABS: 1 ($n = 3$), PP: 24 ($n = 72$), PETE: 8 ($n = 25$), PS: 3 ($n = 12$), PC: 1 ($n = 3$), PLA: 1 ($n = 3$).

3.3.   Country of origin and recycling

We compared $\delta^{13}C$ values from different HDPE bags from major retail stores, produced in Thailand and in the United States (US) (Fig. 3a). The difference between the two countries, about 0.9 ‰ higher for the Thailand bag, suggests that the country of origin (specified on bag) may play a role in the $\delta^{13}C$ value, possibly due to differences in manufacturing processes (e.g., stabilizers, synthesis conditions). Differences between LDPE bags from the US, Thailand, and China were much larger (Fig. 3b). The $\delta^{13}C$ results for US products were about 2–4 ‰ lower relative to a bag from Thailand and 2–5 ‰ lower relative to bags from China. Additional samples are necessary to confirm whether consistent differences exist and, if so, whether they are process related.

Results for PETE items are reported in Fig. 3c. Results (from left to right) correspond to the following items: container (clear), pellets (opaque), container (clear), container (blue, opaque), recycled bottle (clear blue), and a recycled container (clear). All of the clear containers were fruit packaging. Differences between the items are not thought to relate to colorants as the difference between two clear containers (1st and 3rd from left) is greater than that between a clear and blue (opaque) container (3rd and 4th from left, respectively). Results for recycled PETE products were either comparable to or higher than nonrecycled products (Fig. 3c), indicating a difference for a recycled PETE container (fruit packaging) that cannot be determined spectroscopically. The mean $\delta^{13}C$ value for the fruit packaging was 1.1‰ higher than the mean for the nonrecycled PETE samples, which could be explained by the use of bioplastics in the recycling process (e.g., Ref. [57]). The higher $\delta^{13}C$ value for a recycled sample differs from results of a previous study [48], which found a lower mean for recycled PETE samples relative to nonrecycled.

Our $\delta^{13}C$ value for a PP food packaging container made in 2013 is 4 (‰) higher than the values obtained for the 2019 products (Fig. 3d). However, given the different origins of the samples (US and New Zealand), and consequently the potential for different manufacturing processes (temperature, materials, etc.), it is not possible to determine whether both age and geographic origin affected the results. Differences between the other samples, all from the US, were smaller, but these items also could be distinguished based on $\delta^{13}C$ values due to the high measurement precision.

To further address the potential of IRMS for environmental tracking of plastics, plastic straws from 15 suppliers were collected and analyzed, all of which were found to be PP (Figure S-11). Where known, the country of origin was specified, as indicated on the package. As seen in Fig. 4, the $\delta^{13}C$ values varied over a range of − 31.07 to − 24.63 ‰. No trend in the $\delta^{13}C$ values was noted based on country of origin. One straw (orange) from China had a much lower value (− 31.07 ‰) than three others from China. With respect to color, no trend was apparent. For example, the result for a red straw (#10) was closer to that for a white straw (#11) than another red one (#9), and both clear and white straws had a wide range of $\delta^{13}C$ values. The straws likely contained varying levels of plasticizers as some were noticeably more flexible than others. Although no trends for geographic origin or color were noted, based on a two-sample t-test ($p = 0.05$ significance level), statistically significant differences were found between all straws except #12 and #13 ($p = 0.13$). Given the significant differences in the mean $\delta^{13}C$ values, IRMS may be useful for studying

transport of this pervasive plastic debris if the components responsible for these differences are largely retained under environmental conditions.

More generally (beyond straws), IRMS and FTIR/Raman as complementary techniques may allow tracking of some types of plastics. For example, we mention urban sources because most plastic pollution originates from urban areas. Application to regional studies could help identify major sources if isotope signatures are distinguishable and unaltered by environmental conditions. Studies of long-range transport are expected to be more challenging, due to the distance from sources and possible changes in isotope signatures from weathering. However, if an item has a relatively unique signature, small changes may not matter (e. g., if anticipated and isotope signature remains unique). At a minimum, IRMS can indicate whether a plastic is largely petroleum- or plant-derived, or a mixture (e.g. a recycled material). As the industry transitions to more sustainable production processes, isotope signatures for some products may be unique, covering a range that reflects the bio-based materials from which they are derived. As observed for straws, a broad range of differing values may help identify the origins and sources of these materials.

3.4. Polymers aging

Continued weathering/aging can generate secondary N&MPs through breakdown of larger plastic debris. Breakdown occurs through hydrolysis, photodegradation (ultraviolet light), mechanical abrasion, temperature changes, and biological and chemical degradation [58–62], and these environmental stressors can act in concert. For example, prolonged UV exposure causes brittleness due to changes in polymer structure, which increases mechanical degradation [63]. Some polymers are more susceptible to certain stressors than others. In particular, PS and common polyolefins such as PE and PP are more prone to UV breakdown [64–66]. In addition to tracking the geographic origins and source of organic matter in the environment, stable carbon IRMS measurements could be used to mark the changes in polymer structure due environmental weathering/aging, evidenced by increasing $\delta^{13}C$ values as found by Berto et al. [48].

We conducted a preliminary study to examine the short-term exposure effects of common environmental stressors. Fig. 5 presents the IRMS results for plastic items (PP and PS food packaging, white PS foam, and a PETE water bottle) exposed over a one-week period under the following conditions: UV light, UV light + water (stirred at room temperature), water only (30 °C), and heat only (40 °C). The $\delta^{13}C$ means for four samples, a PP candy container, PS foam (white), and two PP yogurt containers (white and clear) showed increases (less negative) relative to unexposed samples, especially for UV exposure. The mean for a PS black food tray also showed an increase, but less than that for a white PS foam sample. The relatively modest increase in the black PS tray may reflect increased stability due to the black additive. Nearly all (22 of 24) of the means were higher for the exposed samples, with statistically significant differences (p = 0.05 significance level) in many cases (Fig. 5). Some results (e.g., for PP white yogurt container and PS white foam) were not significant, likely due to the relatively high uncertainty in the means for unexposed samples. Two results (UV and hot water-light) for a PETE bottle were higher after exposure. Changes in the $\delta^{13}C$ values for PS and PP after UV exposure is expected due to the reported UV sensitivity of

these polymers [64–66]. The trend of increasing values is also consistent with that reported by Berto et al. [48].

3.5. Overview of methods

Infrared and Raman spectroscopy permit identification of polymers and other organic species based on the vibrational frequencies of chemical functional groups. The available techniques have trade-offs with respect to spatial/size resolution, sensitivity, and sample throughput. Advantages of ATR-FTIR include fast, nondestructive analysis; polymer identification (chemical information at a minimum); and little or no sample preparation. Disadvantages include sensitivity to water, manual sample loading, and the relatively large (about 500 μm) particle size required. These limitations were not an issue in our study as we used packaging and other bulk samples (powders/pellets).

Ideally, all suspect N&MPs in a sample should be confirmed analytically [67,68]. However, due to method limitations and time constraints, manual Raman and FTIR methods relied on a relatively small number of particles for MP confirmation. These older methods required manual sorting of particle types under an optical microscope. A subset of particles in each category was then transferred for confirmatory analysis or analyzed directly on a substrate. Particle transfer introduces bias (e.g., missed transparent/small particles) relative to direct spectroscopic analysis [11], and accuracy depends on the number of particles analyzed. The recommended subsampling procedures differ for different size fractions and methods [69]. Results based on small subsets may have considerable uncertainty [70,71]. Micro-FTIR imaging with FPA detection can provide more representative results [27,72,73]. Fast, automated analysis and processing methods that cover a larger sample area can greatly improve particle analysis and have become more common. For example, a μ-FTIR system with an FPA detector can provide automated FTIR imaging of MPs down to about 20 μm [27,72,73].

Relative to μ-FTIR, the main advantage of μ-Raman is higher resolution, important in identifying very small (<20 μm) MPs [39,74–76]. Current generation detectors and fast spectral processing can extend analyses to the sub-μm range. A further advantage is Raman's insensitivity to water, unlike IR measurements. In part, drawbacks such as long measurement times (also true for μ-FTIR) and spectral interference from fluorescence (e.g., of additives or biofilms) have slowed progress on μ-Raman methods. Continuing advancements are expected to resolve these issues and provide even smaller size resolution. Automated analyses can cover a larger sample area (e.g., automated FPA-FTIR), reduce analysis time, and improve data quality. Automated particle selection, Raman (and FTIR) mapping, and comprehensive reference libraries can expedite analyses and improve spectral matching.

Advanced applications such as real-time Raman detection and imaging also may be possible [39]. Gillibert et al. [43] described a Raman instrument that optically traps particles from tens of μm to as small as 90 nm and confirms their chemical composition. It provides particle sizes and shapes and has potential applications to analysis of particles coated with biofilms and other organic substances. The prospects and challenges of Raman and FTIR imaging methods for MPs in environmental samples were reported in a recent review [77]. A

new, automated μ-FTIR method also was reported that accurately (>98%) identified MPs [78]. The method detects and numerically describes vibrational bands by curve fitting, giving a highly characteristic peak list for improved library searches. It is based on a published MP identification algorithm (μIDENT), extended to μ-FTIR data. A recently developed technique called Optical Photothermal IR (O-PTIR) spectroscopy combines IR and Raman spectroscopies in a single instrument that allows simultaneous spectra collection [79]. The technique is based on an IR microscope with a pulsed IR laser (pump) and visible/near IR light (probe) to measure the photothermal response due to IR absorption. It reportedly overcomes limitations of traditional IR spectroscopy, providing high quality spectra in a non-contact reflection mode without scatter/dispersion artifacts, water compatible IR measurements, and IR spatial resolution into the sub-μm range. These emerging measurement tools are expected to advance N&MPs research in a variety of areas including studies of contaminated biological tissues, environmental monitoring, and plastic degradation.

Although FTIR and Raman techniques can identify polymers and possible plastic geographic origins and sources, single particles are required, μ-FTIR has a lower size limit of about 20 μm, and commonly used manual methods are time intensive and subject to bias. Automated methods are expected to reduce the bias and analysis time, but they are not yet widely available and likely to be expensive. A relatively inexpensive, simple method based on Nile red staining and fluorescence was reportedly capable of detecting MPs down to about 3 μm, though μ-fibers could not be stained, and the different types of polymers cannot be distinguished [80]. Nevertheless, depending on the required performance criteria, this relatively simple method may be fit to purpose for some studies.

Unlike spectroscopy, colored additives did not appear to affect the IRMS results. In addition, IRMS can distinguish samples composed of the same polymer when their isotopic signatures differ (e.g., plant- and petroleum-derived plastics). Other advantages include high sensitivity; relatively small sample mass requirement; fast, automated analyses; and low cost. Disadvantages are that IRMS does not identify polymer type, individual or multiple particles of the same type are required, and it is destructive. Thus, when applied to MPs, prior characterization is necessary if the sample amount is insufficient for separate analyses. Another disadvantage relative to spectral analyses is that sample preparation is somewhat tedious and time consuming. However, proper sample preparation, including accurate weighing and careful sample packing, is essential to accuracy and precision. Further, the available sample mass may be a limiting factor in some studies. Analysis of low sample masses (e.g., small particles) may require the modification of a conventional EA-IRMS instrument. Highly precise, accurate measurement of the $\delta^{13}C$ values of μm-sized organic particles traditionally has been limited to secondary ion beam techniques, which are not suitable for analyses of large numbers of individual particles due to the substantial processing time required and instrumental factors (e.g., rough surfaces at the nanometer scale) [51]. Although advances in instrumentation over the last 10 years have greatly reduced the minimum mass of sample required for analysis.

Measurement of the $\delta^{13}C$ values of organic solids has commonly been by EA-IRMS (i.e., combustion in an EA and detection of resulting CO_2 by IRMS). In general, a minimum of

about 20–25 μg of carbon is required, depending on the blank associated with the sample cup and carousel. The use of cleaning protocols and low-blank autosamplers have reduced the blank response. The minimum carbon mass depends on the instrument but at least several micrograms have typically been required [51]. Using a conventional EA-IRMS instrument, the minimum mass was further reduced by decreasing the EA to IRMS split ratio and use of a cryotrap, which allowed measurement of $\delta^{13}C$ values on about 0.5 μg of carbon [51]. New designs can have even lower limits. A design combining laser ablation, nano combustion gas chromatography, and IRMS substantially reduced the lower limit. A deep UV (193 nm) laser allowed optimal fragmentation of organic substances, with minimal isotope fractionation effects. An accuracy and precision better than 0.5‰ were reported for single spot analyses when measuring at least 42 ng of carbon [51]. This approach shows promise for analysis of very small particles, provided individual particles can be isolated.

In some cases, a similar range in isotopic $\delta^{13}C$ values could mask different potential origins and sources, limiting the utility of IRMS. However, multi-element isotope analysis could overcome this limitation. For example, an evaluation of deuterium (D) confirmed its promise in this regard, through source apportionment using mixing models to discriminate between isotopically-overlapping plant types. In a study by Duarte et al. [46]; an overlap was found in the $\delta^{13}C$ and $\delta^{15}N$ values for seagrasses and macroalgae. However, the δD values were significantly different ($- 56.6 \pm 2.8$‰ and $- 95.7 \pm 3.4$‰, respectively). This considerable difference demonstrates the potential of multi-element IRMS for ecological/environmental studies.

4. Conclusions

Our study found IRMS to be a promising tool for tracking the geographic origin and transformations of plastics in the environment. This technique has wide application to many fields. High accuracy and precision at low mass can be achieved. Multi-element analysis could extend the specificity of IRMS in tracing plastic origin, possibly providing information on biofilms. As a complementary technique for plastics characterization, IRMS offers high sensitivity, fast and automated analyses, and low cost. It distinguished plant- and petroleum-derived samples, and samples composed of the same polymer but with different isotope abundances. Colored additives appeared to have no discernible impact on the $\delta^{13}C$ results. Polypropylene straws showed variability in their $\delta^{13}C$ values, possibly due to plasticizers. Additional work is needed to assess the generalizability of our findings. Disadvantages of IRMS are that it does not identify polymer type, single particles or multiple of a given type are required, and it is destructive. Although additives can alter Raman and FTIR spectra, all spectral library matches were accurate. However, known samples were used for the purpose of this study and those did not require pretreatment. Similar studies on field samples would likely require a pretreatment, depending on the sample type.

The $\delta^{13}C$ values for petroleum- and plant-derived polymers reflected these feedstocks, being higher for the latter, consistent with a previous study [48]. Geographic origin may impact the $\delta^{13}C$ values of plastics, possibly due to differences in materials and manufacturing processes. Variability in the $\delta^{13}C$ values for HDPE and LDPE samples was observed, which

may relate to the different geographic origins. Unlike a previous study [48], which found comparable $\delta^{13}C$ values for PETE and recycled PETE, we found differences between two recycled materials, and variability in results for unrecycled samples. The much higher $\delta^{13}C$ result for one of the recycled products may relate to a higher fraction of plant-derived plastics in this product. In addition to its potential for tracking environmental plastics, IRMS could be a useful indicator of polymer age/weathering, based on biotic/abiotic degradation in the environment, but it is especially suited to laboratory studies of polymer degradation under controlled conditions. Studies of interest include investigation of 'biodegradable' polymers and evaluation of new, weather-resistant materials. Our preliminary results indicated a trend of higher $\delta^{13}C$ values for PS and PP items exposed to UV light, consistent with the UV sensitivity of these polymers and a previous study of aged plastics. Further research is needed, regionally and globally, to evaluate the utility of IRMS with confirmatory techniques for investigating the origins, sources, and fate of plastics in the environment.

Supplementary Material

Refer to Web version on PubMed Central for supplementary material.

Acknowledgments

References

[1]. Rochman CM, Brookson C, Bikker J, Djuric N, Earn A, Bucci K, Athey S, Huntington A, McIlwraith H, Munno K, De Frond H, Kolomijeca A, Erdle L, Grbic J, Bayoumi M, Borrelle SB, Wu T, Santoro S, Werbowski LM, Zhu X, Giles RK, Hamilton BM, Thaysen C, Kaura A, Klasios N, Ead L, Kim J, Sherlock C, Ho A, Hung C, Rethinking microplastics as a diverse contaminant suite, Environ. Toxicol. Chem. 38 (4) (2019) 703–711. [PubMed: 30909321]

[2]. Hartmann NB, Huffer T, Thompson RC, Hassellov M, Verschoor A, Daugaard AE, Rist S, Karlsson T, Brennholt N, Cole M, Herrling MP, Hess MC, Ivleva NP, Lusher AL, Wagner M, Are we speaking the same language? Recommendations for a definition and categorization framework for plastic debris, Environ. Sci. Technol. 53 (3) (2019) 1039–1047. [PubMed: 30608663]

[3]. Birch QT, Potter PM, Pinto PX, Dionysiou DD, Al-Abed SR, Sources, transport, measurement and impact of nano and microplastics in urban watersheds, Rev. Environ. Sci. Biotechnol. 19 (2) (2020) 275–336. [PubMed: 32982619]

[4]. Enfrin M, Dumee LF, Lee J, Nano/microplastics in water and wastewater treatment processes - origin, impact and potential solutions, Water Res. 161 (2019) 621–638. [PubMed: 31254888]

[5]. Gatidou G, Arvaniti OS, Stasinakis AS, Review on the occurrence and fate of microplastics in sewage treatment plants, J. Hazard Mater. 367 (2019) 504–512. [PubMed: 30620926]

[6]. Prata JC, Microplastics in wastewater: state of the knowledge on sources, fate and solutions, Mar. Pollut. Bull. 129 (1) (2018) 262–265. [PubMed: 29680547]

[7]. Sun J, Dai XH, Wang QL, van Loosdrecht MCM, Ni BJ, Microplastics in wastewater treatment plants: detection, occurrence and removal, Water Res. 152 (2019) 21–37. [PubMed: 30660095]

[8]. Yang L, Li K, Cui S, Kang Y, An L, Lei K, Removal of microplastics in municipal sewage from China's largest water reclamation plant, Water Res. 155 (2019) 175–181. [PubMed: 30849731]

[9]. Dris R, Gasperi J, Saad M, Mirande C, Tassin B, Synthetic fibers in atmospheric fallout: a source of microplastics in the environment? Mar. Pollut. Bull. 104 (1–2) (2016) 290–293. [PubMed: 26787549]

[10]. Horton AA, Svendsen C, Williams RJ, Spurgeon DJ, Lahive E, Large microplastic particles in sediments of tributaries of the River Thames, UK - abundance, sources and methods for effective quantification, Mar. Pollut. Bull. 114 (1) (2017) 218–226. [PubMed: 27692488]

[11]. Koelmans AA, Nor NHM, Hermsen E, Kooi M, Mintenig SM, De France J, Microplastics in freshwaters and drinking water: critical review and assessment of data quality, Water Res. 155 (2019) 410–422. [PubMed: 30861380]

[12]. Strungaru S-A, Jijie R, Nicoara M, Plavan G, Faggio C, Micro-(nano) plastics in freshwater ecosystems: abundance, toxicological impact and quantification methodology, Trac. Trends Anal. Chem. 110 (2019) 116–128.

[13]. Triebskorn R, Braunbeck T, Grummt T, Hanslik L, Huppertsberg S, Jekel M, Knepper TP, Krais S, Muller YK, Pittroff M, Ruhl AS, Schmieg H, Schur C, Strobel C, Wagner M, Zumbulte N, Kohler HR, Relevance of nano- and microplastics for freshwater ecosystems: a critical review, Trac. Trends Anal. Chem. 110 (2019) 375–392.

[14]. de Sá LC, Oliveira M, Ribeiro F, Rocha TL, Futter MN, Studies of the effects of microplastics on aquatic organisms: what do we know and where should we focus our efforts in the future? Sci. Total Environ. 645 (2018) 1029–1039. [PubMed: 30248828]

[15]. Kershaw P, Sources, Fate and Effects of Microplastics in the Marine Environment: a Global Assessment, 2017.

[16]. Besseling E, Redondo-Hasselerharm P, Foekema EM, Koelmans AA, Quantifying ecological risks of aquatic micro-and nanoplastic, Crit. Rev. Environ. Sci. Technol. 49 (1) (2019) 32–80.

[17]. Curren E, Leong SCY, Profiles of bacterial assemblages from microplastics of tropical coastal environments, Sci. Total Environ. 655 (2019) 313–320. [PubMed: 30471599]

[18]. Li X, Mei Q, Chen L, Zhang H, Dong B, Dai X, He C, Zhou J, Enhancement in adsorption potential of microplastics in sewage sludge for metal pollutants after the wastewater treatment process, Water Res. 157 (2019) 228–237. [PubMed: 30954698]

[19]. Rochman CM, Hoh E, Kurobe T, Teh SJ, Ingested plastic transfers hazardous chemicals to fish and induces hepatic stress, Sci. Rep. 3 (2013).

[20]. Browne MA, Dissanayake A, Galloway TS, Lowe DM, Thompson RC, Ingested microscopic plastic translocates to the circulatory system of the mussel, Mytilus edulis (L), Environ. Sci. Technol. 42 (13) (2008) 5026–5031. [PubMed: 18678044]

[21]. Koelmans AA, Besseling E, Shim WJ, Nanoplastics in the aquatic environment. Critical review, Mar. Anthrop. Litt. (2015) 325–340.

[22]. Parker L, In a first, microplastics found in human poop, J Nat. Geogr. Mag. Online. (2018).

[23]. Conkle JL, Del Valle CDB, Turner JW, Are we underestimating microplastic contamination in aquatic environments? Environ. Manag. 61 (1) (2018) 1–8.

[24]. Cheang CC, Ma Y, Fok L, Occurrence and composition of microplastics in the seabed sediments of the coral communities in proximity of a metropolitan area, Int. J. Environ. Res. Publ. Health 15 (10) (2018).

[25]. Dikareva N, Simon KS, Microplastic pollution in streams spanning an urbanisation gradient, Environ. Pollut. 250 (2019) 292–299. [PubMed: 31003141]

[26]. Gray AD, Wertz H, Leads RR, Weinstein JE, Microplastic in two South Carolina Estuaries: occurrence, distribution, and composition, Mar. Pollut. Bull. 128 (2018) 223–233. [PubMed: 29571367]

[27]. Loder MGJ, Gerdts G, Methodology used for the detection and identification of microplastics-A critical appraisal, Marine Anthropogenic Litter, 2015, pp. 201–227.

[28]. Dumichen E, Eisentraut P, Bannick CG, Barthel AK, Senz R, Braun U, Fast identification of microplastics in complex environmental samples by a thermal degradation method, Chemosphere 174 (2017) 572–584. [PubMed: 28193590]

[29]. Ravit B, Cooper K, Moreno G, Buckley B, Yang I, Deshpande A, Meola S, Jones D, Hsieh A, Microplastics in urban New Jersey freshwaters: distribution, chemical identification, and biological affects, AIMS Environ. Sci. 4 (2017) 809–826.

[30]. Penalver R, Arroyo-Manzanares N, Lopez-Garcia I, Hernandez-Cordoba M, An overview of microplastics characterization by thermal analysis, Chemosphere 242 (2020).

[31]. Lares M, Ncibi MC, Sillanpaa M, Sillanpaa M, Occurrence, identification and removal of microplastic particles and fibers in conventional activated sludge process and advanced MBR technology, Water Res. 133 (2018) 236–246. [PubMed: 29407704]

[32]. Leslie HA, Brandsma SH, van Velzen MJM, Vethaak AD, Microplastics en route: field measurements in the Dutch river delta and Amsterdam canals, wastewater treatment plants, North Sea sediments and biota, Environ. Int. 101 (2017) 133–142. [PubMed: 28143645]

[33]. Luo W, Su L, Craig NJ, Du F, Wu C, Shi H, Comparison of microplastic pollution in different water bodies from urban creeks to coastal waters, Environ. Pollut. 246 (2019) 174–182. [PubMed: 30543943]

[34]. Magni S, Binelli A, Pittura L, Avio CG, Della Torre C, Parenti CC, Gorbi S, Regoli F, The fate of microplastics in an Italian wastewater treatment plant, Sci. Total Environ. 652 (2019) 602–610. [PubMed: 30368189]

[35]. Bordos G, Urbanyi B, Micsinai A, Kriszt B, Palotai Z, Szabo I, Hantosi Z, Szoboszlay S, Identification of microplastics in fish ponds and natural freshwater environments of the Carpathian basin, Europe, Chemosphere 216 (2019) 110–116. [PubMed: 30359912]

[36]. Kappler A, Fischer M, Scholz-Bottcher BM, Oberbeckmann S, Labrenz M, Fischer D, Eichhorn KJ, Voit B, Comparison of mu-ATR-FTIR spectroscopy and py-GCMS as identification tools for microplastic particles and fibers isolated from river sediments, Anal. Bioanal. Chem. 410 (21) (2018) 5313–5327. [PubMed: 29909455]

[37]. Su L, Cai HW, Kolandhasamy P, Wu CX, Rochman CM, Shi HH, Using the Asian clam as an indicator of microplastic pollution in freshwater ecosystems, Environ. Pollut. 234 (2018) 347–355. [PubMed: 29195176]

[38]. Anger PM, von der Esch E, Baumann T, Elsner M, Niessner R, Ivleva NP, Raman microspectroscopy as a tool for microplastic particle analysis, Trac. Trends Anal. Chem. 109 (2018) 214–226.

[39]. Araujo CF, Nolasco MM, Ribeiro AMP, Ribeiro-Claro PJA, Identification of microplastics using Raman spectroscopy: latest developments and future prospects, Water Res. 142 (2018) 426–440. [PubMed: 29909221]

[40]. Harrison JP, Ojeda JJ, Romero-Gonzalez ME, The applicability of reflectance micro-Fourier-transform infrared spectroscopy for the detection of synthetic microplastics in marine sediments, Sci. Total Environ. 416 (2012) 455–463. [PubMed: 22221871]

[41]. Schwaferts C, Niessner R, Elsner M, Ivleva NP, Methods for the analysis of submicrometer- and nanoplastic particles in the environment, Trac. Trends Anal. Chem. 112 (2019) 52–65.

[42]. Blair RM, Waldron S, Phoenix VR, Gauchotte-Lindsay C, Microscopy and elemental analysis characterisation of microplastics in sediment of a freshwater urban river in Scotland, UK, Environ. Sci. Pollut. Res. Int. 26 (12) (2019) 12491–12504. [PubMed: 30848429]

[43]. Gillibert R, Balakrishnan G, Deshoules Q, Tardivel M, Magazzu A, Donato MG, Marago OM, Lamy M de La Chapelle, Colas F, Lagarde F, Gucciardi PG, Raman tweezers for small microplastics and nanoplastics identification in seawater, Environ. Sci. Technol. (2019).

[44]. Amenabar I, Poly S, Goikoetxea M, Nuansing W, Lasch P, Hillenbrand R, Hyperspectral infrared nanoimaging of organic samples based on Fourier transform infrared nanospectroscopy, Nat. Commun. 8 (2017) 14402. [PubMed: 28198384]

[45]. Muccio Z, Jackson GP, Isotope ratio mass spectrometry, Analyst 134 (2) (2009) 213–222. [PubMed: 19173039]

[46]. Duarte CM, Delgado-Huertas A, Anton A, Carrillo-de-Albornoz P, López-Sandoval DC, Agustí S, Almahasheer H, Marbá N, Hendriks IE, Krause-Jensen D, Stable Isotope (δ13C, δ15N, δ18O, δD) Composition and Nutrient Concentration of Red Sea Primary Producers, 2018.

[47]. Berto D, Rampazzo F, Gion C, Noventa S, Formalewicz M, Ronchi F, Traldi U, Giorgi G, Plastics in the Environment, 2019 (IntechOpen).

[48]. Berto D, Rampazzo F, Gion C, Noventa S, Ronchi F, Traldi U, Giorgi G, Cicero AM, Giovanardi O, Preliminary study to characterize plastic polymers using elemental analyser/isotope ratio mass spectrometry (EA/IRMS), Chemosphere 176 (2017) 47–56. [PubMed: 28254714]

[49]. Suzuki Y, Akamatsu F, Nakashita R, Korenaga T, A novel method to discriminate between plant- and petroleum-derived plastics by stable carbon isotope analysis, Chem. Lett. 39 (9) (2010) 998–999.

[50]. Faure G, Mensing TM, Principles and Applications, John Wiley & Sons, Inc, 2005.

[51]. van Roij L, Sluijs A, Laks JJ, Reichart GJ, Stable carbon isotope analyses of nanogram quantities of particulate organic carbon (pollen) with laser ablation nano combustion gas chromatography/ isotope ratio mass spectrometry, Rapid Commun. Mass Spectrom. 31 (1) (2017) 47–58. [PubMed: 27766694]

[52]. Machavaram M, Mills M, NRMRL LRPCD SOP for 13C and/or 15N isotope ratio analyses of environmental samples (solid and non-aqueous liquid), in: Elemental Analyzer - Isotope Ratio Mass-Spectrometer (EA-IRMS), 2017 EPA (ed).

[53]. Coplen TB, Guidelines and recommended terms for expression of stable-isotoperatio and gas-ratio measurement results, Rapid Commun. Mass Spectrom. 25 (17) (2011) 2538–2560. [PubMed: 21910288]

[54]. Jung MR, Horgen FD, Orski SV, Rodriguez CV, Beers KL, Balazs GH, Jones TT, Work TM, Brignac KC, Royer SJ, Hyrenbach KD, Jensen BA, Lynch JM, Validation of ATR FT-IR to identify polymers of plastic marine debris, including those ingested by marine organisms, Mar. Pollut. Bull. 127 (2018) 704–716. [PubMed: 29475714]

[55]. Talvitie J, Mikola A, Koistinen A, Setala O, Solutions to microplastic pollution - removal of microplastics from wastewater effluent with advanced wastewater treatment technologies, Water Res. 123 (2017) 401–407. [PubMed: 28686942]

[56]. Scientific TF, Guide to the identification of microplastics by FT-IR and Raman spectroscopy, Thermo Fisher Sci. White Pap. WP53077 (2018).

[57]. Wojnowska-Baryla I, Kulikowska D, Bernat K, Effect of bio-based products on waste management, Sustainability 12 (5) (2020).

[58]. Barnes DK, Galgani F, Thompson RC, Barlaz M, Accumulation and fragmentation of plastic debris in global environments, Philos. Trans. R. Soc. Lond. B Biol. Sci. 364 (1526) (2009) 1985–1998. [PubMed: 19528051]

[59]. Browne MA, Crump P, Niven SJ, Teuten E, Tonkin A, Galloway T, Thompson R, Accumulation of microplastic on shorelines worldwide: sources and sinks, Environ. Sci. Technol. 45 (21) (2011) 9175–9179. [PubMed: 21894925]

[60]. Imhof HK, Schmid J, Niessner R, Ivleva NP, Laforsch C, A novel, highly efficient method for the separation and quantification of plastic particles in sediments of aquatic environments, Limnol Oceanogr. Methods 10 (2012) 524–537.

[61]. Lehner R, Weder C, Petri-Fink A, Rothen-Rutishauser B, Emergence of nanoplastic in the environment and possible impact on human health, Environ. Sci. Technol. 53 (4) (2019) 1748–1765. [PubMed: 30629421]

[62]. Thompson RC, Olsen Y, Mitchell RP, Davis A, Rowland SJ, John AWG, McGonigle D, Russell AE, Lost at sea: where is all the plastic? Science 304 (5672) (2004) 838–838. [PubMed: 15131299]

[63]. Mattsson K, Hansson LA, Cedervall T, Nano-plastics in the aquatic environment, Environ. Sci. Process. Impacts 17 (10) (2015) 1712–1721. [PubMed: 26337600]

[64]. Feldman D, Weathering of polymers, 1983, in: Davis A, Sims D (Eds.), Applied Science Publishers, London, 1984, p. 294 Price: $64.75. Journal of Polymer Science: Polymer Letters Edition 22(7), 423–423.

[65]. Gijsman P, Hennekens J, Janssen K, ACS Publications, 1996.

[66]. Song YK, Hong SH, Jang M, Han GM, Jung SW, Shim WJ, Combined effects of UV exposure duration and mechanical abrasion on microplastic fragmentation by polymer type, Environ. Sci. Technol. 51 (8) (2017) 4368–4376. [PubMed: 28249388]

[67]. Dyachenko A, Mitchell J, Arsem N, Extraction and identification of microplastic particles from secondary wastewater treatment plant (WWTP) effluent, Anal. Methods 9 (9) (2017) 1412–1418.

[68]. Tagg AS, Sapp M, Harrison JP, Ojeda JJ, Identification and quantification of microplastics in wastewater using focal plane array-based reflectance micro-FT-IR imaging, Anal. Chem. 87 (12) (2015) 6032–6040. [PubMed: 25986938]

[69]. Mintenig SM, Bauerlein PS, Koelmans AA, Dekker SC, Van Wezel A, Closing¨ the gap between small and smaller: towards a framework to analyse nano-and microplastics in aqueous environmental samples, Environ. Sci.: Nano 5 (7) (2018) 1640–1649.

[70]. Burns EE, Boxall ABA, Microplastics in the aquatic environment: evidence for or against adverse impacts and major knowledge gaps, Environ. Toxicol. Chem. 37 (11) (2018) 2776–2796. [PubMed: 30328173]

[71]. Hermsen E, Mintenig SM, Besseling E, Koelmans AA, Quality criteria for the analysis of microplastic in biota samples: a critical review, Environ. Sci. Technol. 52 (18) (2018) 10230–10240. [PubMed: 30137965]

[72]. Primpke S, Lorenz C, Rascher-Friesenhausen R, Gerdts G, An automated approach for microplastics analysis using focal plane array (FPA) FTIR microscopy and image analysis, Anal. Methods 9 (9) (2017) 1499–1511.

[73]. Simon M, van Alst N, Vollertsen J, Quantification of microplastic mass and removal rates at wastewater treatment plants applying Focal Plane Array (FPA)- based Fourier Transform Infrared (FT-IR) imaging, Water Res. 142 (2018) 1–9. [PubMed: 29804032]

[74]. Elert AM, Becker R, Duemichen E, Eisentraut P, Falkenhagen J, Sturm H, Braun U, Comparison of different methods for MP detection: what can we learn from them, and why asking the right question before measurements matters? Environ. Pollut. 231 (2017) 1256–1264. [PubMed: 28941715]

[75]. Ivleva NP, Wiesheu AC, Niessner R, Microplastic in aquatic ecosystems, Angew. Chem. Int. Ed. 56 (7) (2017) 1720–1739.

[76]. Kappler A, Fischer D, Oberbeckmann S, Schernewski G, Labrenz M, Eichhorn KJ, Voit B, Analysis of environmental microplastics by vibrational microspectroscopy: FTIR, Raman or both? Anal. Bioanal. Chem. 408 (29) (2016) 8377–8391. [PubMed: 27722940]

[77]. Xu JL, Thomas KV, Luo ZS, Gowen AA, FTIR and Raman imaging for microplastics analysis: state of the art, challenges and prospects, Trac. Trends Anal. Chem. 119 (2019).

[78]. Renner G, Sauerbier P, Schmidt TC, Schram J, Robust automatic identification of microplastics in environmental samples using FTIR microscopy, Anal. Chem. 91 (15) (2019) 9656–9664. [PubMed: 31287674]

[79]. Marcott C, Kansiz M, Dillon E, Cook D, Mang MN, Noda I, Two-dimensional correlation analysis of highly spatially resolved simultaneous IR and Raman spectral imaging of bioplastics composite using optical photothermal Infrared and Raman spectroscopy, J. Mol. Struct. 1210 (2020).

[80]. Wiggin KJ, Holland EB, Validation and application of cost and time effective methods for the detection of 3–500mum sized microplastics in the urban marine and estuarine environments surrounding Long Beach, California, Mar. Pollut. Bull. 143 (2019) 152–162. [PubMed: 31789151]
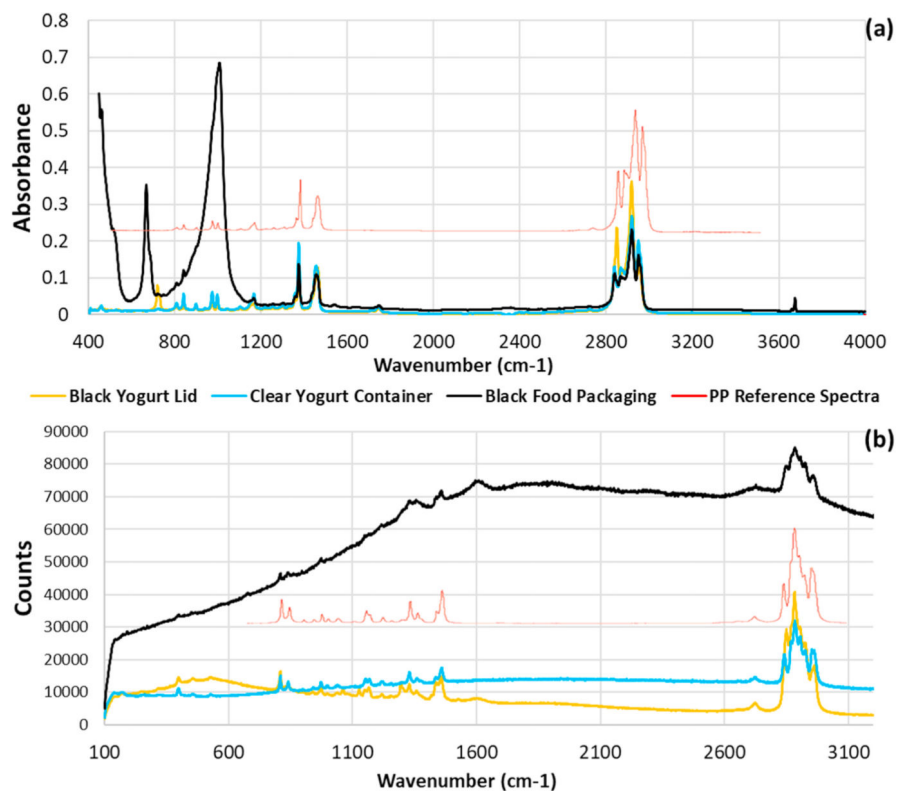
Fig. 1.
Spectral differences in FTIR (a) and Raman (b) microscopy due to dark additive(s) in PP items. The ATR-FTIR spectra (a) show additional peaks from the additive(s), while the Raman result for a black food packaging had high background. In both cases, characteristic peaks for PP are present. (reference spectra from Thermo Fisher [56].
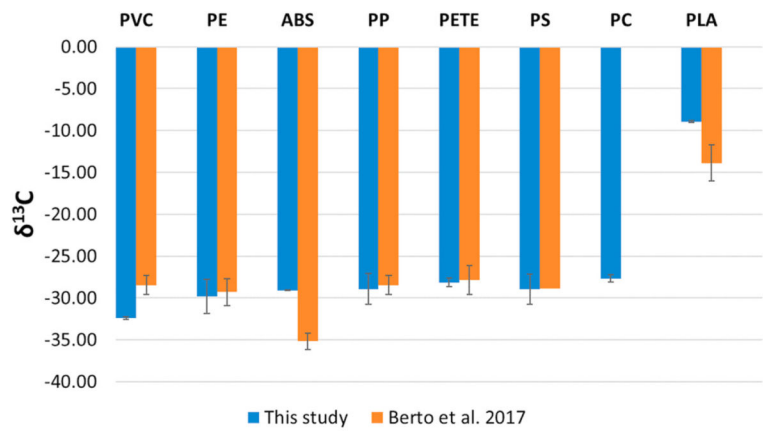
Fig. 2.
Comparison of IRMS results (means) from this study and Berto et al. [48]. Error bars indicate standard deviation.
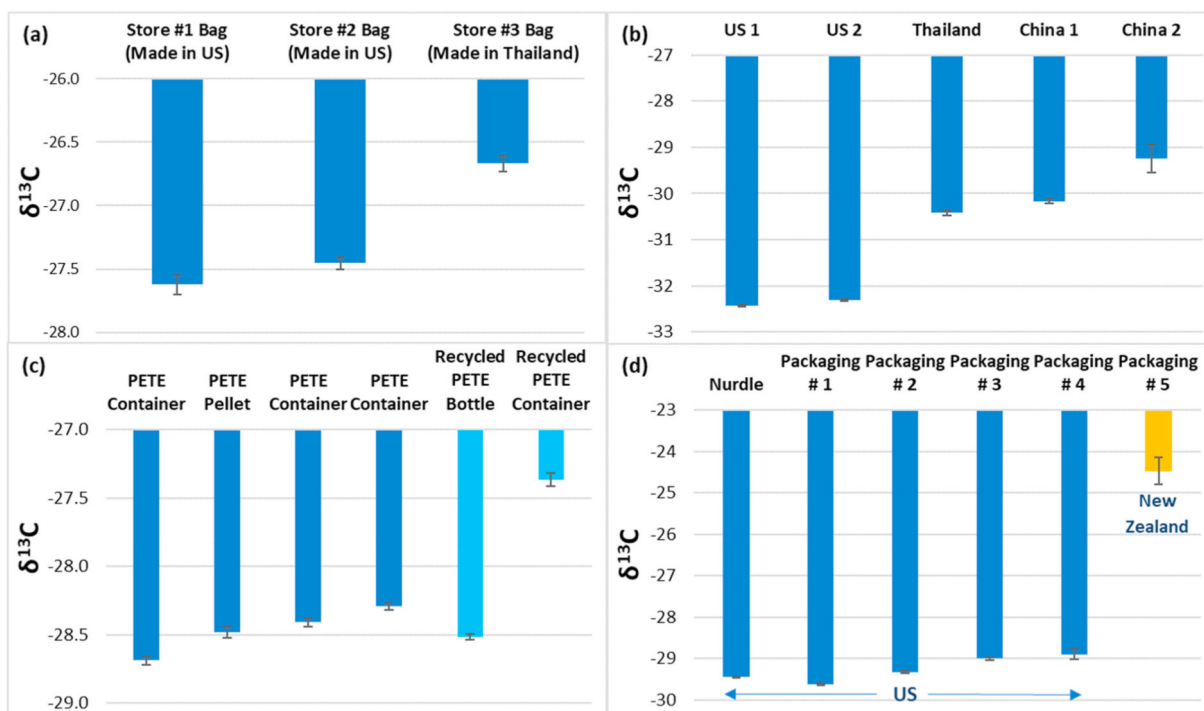
Fig. 3.

IRMS results for plastic items of different geographical origin and for nonrecycled and recycled products. Results are for individual items of the following: a) HDPE disposable bags, b) LDPE bags, c) PETE and recycled PETE items, and d) PP food packaging/ containers. All PP samples from the United States (US) were made in 2019, while a container from New Zealand was dated 2013. Bars and error bars are means (n = 3 or 4) and standard deviations. See text for additional details.
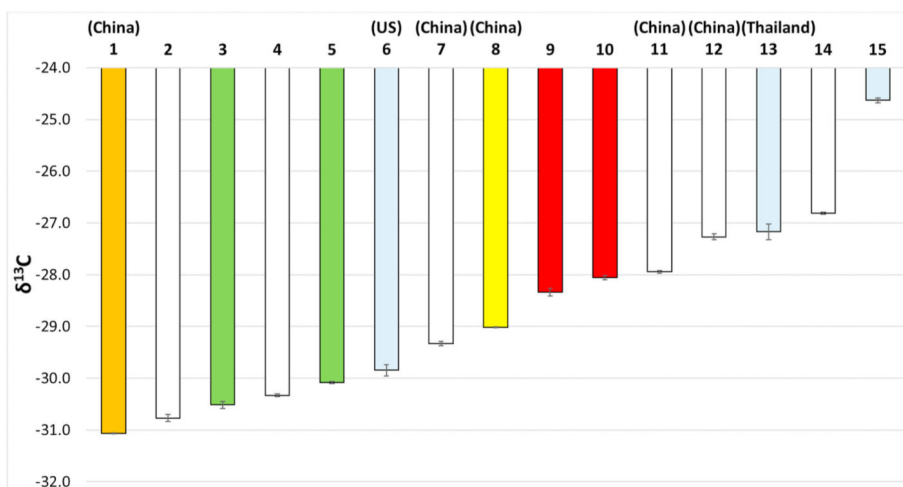
Fig. 4.

$\delta^{13}C$ results (n = 3) for 15 plastic straws of different geographic origins (specified where known). The bar colors indicate the colors of the straws, with grey representing a clear material. See text for details.
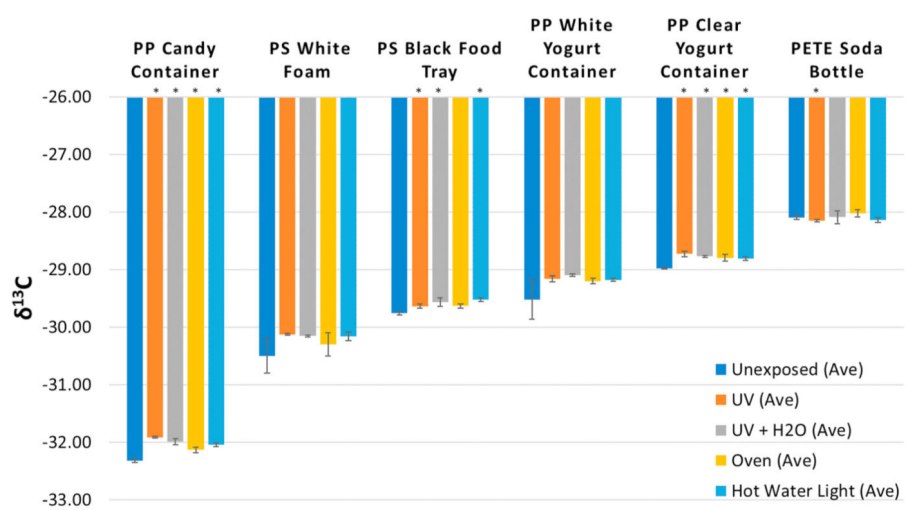
Fig. 5.
Mean $\delta^{13}C$ results ($n = 3$) for plastic packaging items before and after exposure to different environmental stressors (simulated conditions). Error bars indicate standard deviation. Asterisks indicate statistically significant differences based on *t*-test (see Supplemental Information for details).